

# FInC Flow: Fast and Invertible $k \times k$ Convolutions for Normalizing Flows

Aditya Kallappa, Sandeep Nagar and Girish Varma  
International Institute of Information Technology, Hyderabad, India

Keywords: Normalizing Flows, Deep Learning, Invertible Convolutions.

Abstract: Invertible convolutions have been an essential element for building expressive normalizing flow-based generative models since their introduction in Glow. Several attempts have been made to design invertible  $k \times k$  convolutions that are efficient in training and sampling passes. Though these attempts have improved the expressivity and sampling efficiency, they severely lagged behind Glow which used only  $1 \times 1$  convolutions in terms of sampling time. Also, many of the approaches mask a large number of parameters of the underlying convolution, resulting in lower expressivity on a fixed run-time budget. We propose a  $k \times k$  convolutional layer and Deep Normalizing Flow architecture which i.) has a fast parallel inversion algorithm with running time  $O(nk^2)$  ( $n$  is height and width of the input image and  $k$  is kernel size), ii.) masks the minimal amount of learnable parameters in a layer. iii.) gives better forward pass and sampling times comparable to other  $k \times k$  convolution-based models on real-world benchmarks. We provide an implementation of the proposed parallel algorithm for sampling using our invertible convolutions on GPUs. Benchmarks on CIFAR-10, ImageNet, and CelebA datasets show comparable performance to previous works regarding bits per dimension while significantly improving the sampling time.

## 1 INTRODUCTION

Normalizing flow is an important subclass of Deep Generative Models that offers distinctive benefits (Kobyzev et al., 2020). In comparison to GANs (Goodfellow et al., 2014a) and VAEs (Kingma et al., 2019), they are trained using a very intuitive Maximum Likelihood loss function. Images and the *latent vector*, which is required to have a Gaussian distribution, correspond one-to-one in flow models. Despite these intriguing characteristics, GANs and VAEs are utilized more frequently. This is due to the need for the Normalizing Flows transformations to be invertible, which significantly restricts the neural network types employed. For deployment in a real-world scenario, the invertible transformations must be efficiently calculable in the forward and sample stages.

A significant breakthrough came with Glow (Kingma and Dhariwal, 2018) which used  $1 \times 1$  invertible convolutions to design normalizing flows. If it exists, the inverse function for a  $1 \times 1$  convolution also happens to be a  $1 \times 1$  convolution. Since computing  $1 \times 1$  convolution has fast parallel algorithms for which running time does not depend on the spatial dimensions, they are also highly efficient in forward pass (i.e. computing *latent vector* from an image) as

well as the sampling passes (i.e. computing image from a sampled *latent vector*). Extending Glow to use invertible  $k \times k$  convolutions promises to improve the expressivity further, allowing it to model more complex datasets. However, this is a challenging problem since the inverse function for a  $k \times k$  convolution, in general, is given by a  $n^2 \times n^2$  matrix where  $n = H = W$  (i.e. the spatial dimensions). Hence, while the forward pass can be fast, the trivial approach for the sampling pass will cost  $O(n^4)$  operations per convolutional layer.

CInC Flow (Nagar et al., 2021) introduced a padded  $3 \times 3$  convolution layer design and gave it the necessary and sufficient conditions to make it invertible. They showed that the convolution matrix is lower triangular by ensuring padding in only two sides of the input. Furthermore, all the diagonal entries of the convolution matrix are equal to a single weight parameter. By setting this parameter to 1, they ensured that the convolutions are invertible, and Jacobian is always 1.

We build on their work by proposing a parallel inversion algorithm for their convolution design. The parallel algorithm only uses  $O(nk^2)$  sequential operations, unlike  $O(n^2k^2)$  operations used by most previous works. We also build a normalizing flow archi-

The figure illustrates the convolution process as a linear transformation. On the left, a  $3 \times 3$  padded input matrix  $X^{(TL)}$  is shown with zeros in the top-left corner and input pixels  $x_{11}, x_{12}, x_{13}$  in the top row,  $x_{21}, x_{22}, x_{23}$  in the middle row, and  $x_{31}, x_{32}, x_{33}$  in the bottom row. This is multiplied by a  $2 \times 2$  kernel matrix with weights  $w_{11}, w_{12}$  in the top row and  $w_{21}, w_{22}$  in the bottom row. The result is a  $10 \times 10$  convolution matrix  $\mathbf{M}$  and a  $10 \times 1$  vectorized input  $x$ . The matrix  $\mathbf{M}$  is lower triangular, with diagonal elements corresponding to the kernel weights. The rows of  $\mathbf{M}$  are color-coded to show dependencies: the first row (red) depends only on  $x_{11}$ ; the second row (green) depends on  $x_{11}, x_{12}$ ; the third row (yellow) depends on  $x_{11}, x_{12}, x_{13}$ ; the fourth row (light blue) depends on  $x_{11}, x_{12}, x_{21}$ ; the fifth row (blue) depends on  $x_{11}, x_{12}, x_{21}, x_{22}$ ; the sixth row (purple) depends on  $x_{11}, x_{12}, x_{21}, x_{22}, x_{23}$ ; the seventh row (dark blue) depends on  $x_{11}, x_{12}, x_{21}, x_{22}, x_{31}$ ; the eighth row (cyan) depends on  $x_{11}, x_{12}, x_{21}, x_{22}, x_{31}, x_{32}$ ; the ninth row (teal) depends on  $x_{11}, x_{12}, x_{21}, x_{22}, x_{31}, x_{32}, x_{33}$ ; and the tenth row (light green) depends on  $x_{11}, x_{12}, x_{21}, x_{22}, x_{31}, x_{32}, x_{33}$ .

Figure 1: Convolution of a  $3 \times 3$  TL (Top Left) padded image with a  $2 \times 2$  filter viewed as a linear transform of vectorized input( $x$ ) by the convolution matrix  $\mathbf{M}$ . The TL padding on the input results in the making matrix  $\mathbf{M}$  lower triangular, and all diagonal values correspond to  $w_{k,k}$  of the filter. Each row of  $\mathbf{M}$  can be used to find a pixel value. The rows or pixels with the same color can be inverted in parallel since all the other values required for computing them will already be available at a step of our inversion algorithm 1.

ture, where channel-wise splitting is further used to parallelize operations.

### Our Contributions.

1. We design a  $k \times k$  invertible convolutional layer with a fast and parallel invertible sampling algorithm (see Sections 4.1, 4.2).
2. We build a normalizing flow architecture based on the fast invertible convolution, which uses channel wise splitting to improve the parallelism further (see Sections 4.3, 4.4).
3. We provide a fast GPU implementation of our parallel inversion algorithm and benchmark the sampling times of the model (see Section 5). We show greatly improved sampling times due to our parallel inversion algorithm, while giving similar bits per dimensions as compared to other works.

## 2 RELATED WORK

**Generative Modeling.** The idea of generative modeling stems from training a generative model whose sample comes from the same distribution as the training data distribution. Most of the generative models can be grouped as Generative adversarial networks (GANs) (Goodfellow et al., 2014b; Brock et al., 2019), Energy-based models (EBMs) (Zhang et al., 2022; Song et al., 2021a), Variational autoencoders (VAEs) (Kingma and Welling, 2013; Kingma et al., 2019; Hazami et al., 2022), Autoregressive models (Oord et al., 2016; Nash et al., 2020), Diffusion models (Ho et al., 2020; Song et al., 2021b; Song and Ermon, 2019) and Flow-based models (Dinh et al., 2014, 2017; Hooeboom et al., 2019; Kingma and Dhariwal, 2018; Ho et al., 2019; Ma et al., 2019; Nagar et al., 2021).

**Normalizing Flows.** Flows-based models construct complex distributions by transforming a probability density through a series of invertible mappings (Rezende and Mohamed, 2015). At the end of these invertible mapping, we obtain a valid distribution; hence, this type of flow is referred to as a Normalizing Flow model. Flow models apply the rule for change of variables; the initial density ‘flows’ through the sequence of invertible mappings (Dinh et al., 2017). Flow-based models generalize a dataset distribution into a latent space (Kobyzev et al., 2020).

**Invertible  $k \times k$  Convolutions.** An invertible neural network requires the inverse of the network with fast and efficient computation of the Jacobian determinant (Song et al., 2019). An invertible neural network can be used for generation and classification with more interpretability. (Kingma and Dhariwal, 2018) proposed an invertible  $1 \times 1$  convolution building on top of NICE (Dinh et al., 2014) and RealNVP (Dinh et al., 2017) consisting a series of flow step combined in a multi-scale architecture. Each flow step consists of actnorm followed by an invertible  $1 \times 1$  convolution, followed by a coupling layer (see Sec 4.3). Emerging (Hooeboom et al., 2019) presented method to generalized  $1 \times 1$  convolution to invertible  $k \times k$  convolutions. Emerging chains two specific autoregressive convolutions (Kingma and Welling, 2013) to form a single convolutional layer following the associativity of the convolution operation. Each of these autoregressive convolutions is chosen such that the resulting convolution matrix  $\mathbf{M}$  is triangular with an inverse time of each of the convolutions is  $O(n \times n \times k^2)$ . MintNet (Song et al., 2019) presented a method for designing invertible neural networks by combining building blocks with a set of composition rules. The inversion of the proposed blocks necessitates a sequence of dependent computations that increase the

Table 1: Comparison of the learnable parameters. where  $n \times n$  is input size,  $k \times k$  is filter size which is constant,  $c$  is number of input/output channels.  $d$  is the number of latent dimensions. # of ops: required number of operations for the inversion of convolutional layers. The complexity of Jacobian: Time complexity for calculating the Jacobian of a single convolution layer. For FInC Flow and CInC Flow, the Jacobian is 1, since the Convolution matrix is lower triangular with diagonal entries being 1.

Method	# of ops	# params / CNN layer	Complexity of Jacobian	Inverse
FInC Flow (our)	$(2n - 1)k^2$	$k^2 - 1$	1	exact
Woodbury (Lu and Huang, 2020)	$cn^2$	$k^2$	$O(d^2(c + n) + d^3)$	exact
MaCow (Ma et al., 2019)	$4nk^2$	$k(\lceil \frac{k}{2} \rceil - 1)$	$O(n^3)$	exact
Emerging (Hoogetboom et al., 2019)	$2n^2k^2$	$k(\lceil \frac{k}{2} \rceil - 1)$	$O(n)$	exact
CInC Flow (Nagar et al., 2021)	$n^2k^2$	$k^2 - 1$	1	exact
MintNet (Song et al., 2019)	$3n$	$\frac{k^2}{3}$	$O(n)$	approx
SNF (Keller et al., 2021)	$k^2$	$k^2$	approx	approx

network’s sampling time. SNF (Keller et al., 2021) proposed a method to reduce the computation complexity of the Jacobian determinant by replacing the gradient term with a learned approximate inverse for each layer. This method avoids the determinant of Jacobian and makes it approximate, and requires an additional backward pass for inversion of convolution. MaCow (Ma et al., 2019) while many other papers make use of the invertibility of triangular matrix to reduce inversion time, MaCow outperforms all of them by performing the inverse in  $O(nk^2)$  by carefully masking 4 kernels at the top, left, bottom, right to achieve a full convolution, but this flow model use four autoregressive convolutions to make an effective standard convolution. Woodbury (Lu and Huang, 2020) this paper employs the *Woodbury transformation* for invertible convolution, which is a generalized permutation layer that models dimension dependencies along the channel and spatial axes using the channel and spatial transformation. ButterflyFlow (Meng et al., 2022) introduced a new family of an invertible layer that works for special underlying structures and needs a sequence of layers for an effective invertible convolution.

**Fast Algorithms for Invertible Convolutions.** CInC Flow (Nagar et al., 2021), derive necessary and sufficient conditions on a padded CNN for it to be invertible and require a single CNN layer for every effective invertible CNN layer. The padded CNN can leverage the advantage of parallel computation for inversion, resulting in faster and more efficient computation of Jacobian determinants.

The distinguishing feature of our invertible convolutions as compared to previous works is that we have a parallel inversion algorithm that does only  $(2n - 1)k^2$  operations where  $n$  is input size and  $k$  is kernel size. MaCow is the closest approach that takes twice the number of operations. Some of the ap-

proaches, like MintNet and SNF, do achieve a lesser number of operations. However, they are not proper normalizing flows as they compute only an approximate inverse. We use the convolution design from CInC Flow but give a parallel inversion algorithm for it. Furthermore, our FInC Flow *Unit* is designed to efficiently parallelize the operations by splitting the convolution operations channel-wise. In Table 1, we compare our proposed flow model with the existing model in terms of the receptive fields/number of learnable parameters, complexity of computing the inverse of convolution layer for sampling.

### 3 PRELIMINARIES

**Normalizing Flows.** Formally, Normalizing Flows is a series of transformations of a known simple probability density into a much more complex probability density using invertible and differentiable functions. These invertible function allows to write the probability of the output as a differentiable function of the model parameters. As a result, the models can be trained using backpropagation with the negative log likelihood loss function.

Let  $\mathbf{X} \in \mathbb{R}^d$  be a random variable with tractable density  $p_{\mathbf{X}}$ . Let  $f : \mathbb{R}^d \rightarrow \mathbb{R}^d$  be a differentiable and invertible function. If  $\mathbf{Y} = f(\mathbf{X})$  then the density of  $Y$  can be calculated as

$$p_Y(y) = p_X(x) |\det J_f| \quad \text{where} \quad J_f = \frac{\partial f(x)}{\partial x}.$$

Note that  $J_f$  is a  $d \times d$  matrix called the Jacobian. If  $X$  is transformed using a sequence of functions  $f_i$ ’s. That is  $f = f_1 \circ f_2 \circ f_3 \circ \dots \circ f_r$ . Now probability density,  $p_Y(y)$  can be expressed as

$$p_Y(y) = p_X(f^{-1}(y)) \cdot \prod_{i=r}^1 |J_{f_i^{-1}}(y_i)|. \quad (1)$$

where  $y_i = f_i^{-1} \circ \dots \circ f_r^{-1}(x)$ . The log-probability of  $p_Y$  which will be used to model the complex image distribution is given by,

$$\log p_Y(y) = \log p_X(f^{-1}(y_r)) + \sum_{i=1}^r \log |\det J_{f_i^{-1}}(y_i)|. \quad (2)$$

The functions  $f_i^{-1}$  will be given by neural network layers and the above function can be computed during the forward pass of the neural network. The negative of this function called the negative log likelihood (NLL) is minimized when images in the dataset are given highest probabilities. Hence it gives a simple, interpretable loss function for training the model.

**Invertible Convolutions.** The convolution of an input  $X$  with shape  $H \times W \times C$  with a kernel  $K$  with shape  $k \times k \times C \times C$  is  $Y = X \times K$  of shape  $(H - (k + 1)) \times (W - (k + 1)) \times C$  which is equal to

$$Y_{i,j,c_0} = \sum_{l,h < k} \sum_{c_i=1}^C X_{i+l,j+h,c_i} K_{l,k,c_i,c_0} \quad (3)$$

Notice that the dimensions of  $X$  and  $Y$  are not necessarily the same. To ensure that the  $X$  and  $Y$  are the same size, we apply padding to the input  $X$ . For an input image  $X$  with shape  $H \times W \times C$ , the  $(t, b, l, r)$  padding of  $X$  is the image  $\hat{X}$  of shape  $(H + t + b) \times (W + l + r) \times C$  is defined as

$$\hat{X}_{i,j,c} = \begin{cases} X_{i-t,j-l,c} & \text{if } i-t < H \text{ and } j-l < W \\ 0 & \text{otherwise} \end{cases} \quad (4)$$

The convolution operation is a linear transformation of the input. For the vectored (flattened) input  $X$ , denoted by  $x$ , the output vector  $y$  can be written as  $y = \mathbf{M}x$ . Matrix  $\mathbf{M}$  is called as the *Convolution Matrix* and the dimensions of this matrix is  $HWC \times HWC$ . As long as matrix  $\mathbf{M}$  is invertible, the convolutional layer can be included as a part of the Normalizing Flows. The common approach to building invertible convolutions is by making  $M$  upper triangular and ensuring invertibility by making diagonal entries to be nonzero.

**Algorithms for Computing Inverse of Convolutions.** For normalizing flows built using invertible convolutions, the sampling pass will involve computing the inverse of the convolution matrix. This involves solving a linear systems of equations  $\mathbf{M}x = y$ .

For a general square matrix of size  $n \times n$ , the time complexity for inversion is  $O(n^3)$ . For a lower triangular matrix of size  $n \times n$ , the time complexity for inversion is  $O(n^2)$  because of back-substitution method. Notice that the size of convolution matrix,

$\mathbf{M}$  is  $n^2 \times n^2$  (refer Figure 1) and also that row of the matrix has only  $k^2$  entries at the maximum, results in an inversion time of  $O(n^2k^2)$  which is used in many of the previous works like Emerging and CInC Flows. We show that this method can be parallelized for carefully designed convolutions giving a complexity of only  $O(nk^2)$ .

## 4 FInC FLOW: OUR APPROACH

In this section we describe our approach including convolution layer design which has a fast parallel inversion algorithm with running time  $O(nk^2)$ . For more clarity, we refer to height of the image as  $H$ , width as  $W$  and channels as  $C$  in this section.

### 4.1 Convolution Design

As it is obvious from equation  $x = \mathbf{M}^{-1}y$ , the inverse timings depends on  $\mathbf{M}$ . Emerging (Behrmann et al., 2019) masks almost half of the convolution kernel values to ensure  $\mathbf{M}$  is a Lower Triangular Matrix. However, we follow the method followed in CInC Flow, where only a few values of the convolution kernel are masked. For an input image  $X$  with shape  $H \times W \times C$ , the top-left (TL) i.e.,  $(t, 0, l, 0)$  padding of  $X$  is the image  $X^{(TL)}$  of shape  $(H + t) \times (W + l) \times C$  is defined in equation 5 and similarly for the top-right (TR) as equation 6, bottom-left (BL) as equation 7, bottom-right (BR) as equation 8.

$$X_{i,j,c}^{(TL)} = \begin{cases} X_{i-t,j-l,c} & i-t > 0 \wedge j-l > 0 \\ 0 & \text{otherwise} \end{cases} \quad (5)$$

$$X_{i,j,c}^{(TR)} = \begin{cases} X_{i-t,j,c} & i-t > 0 \wedge j-r < W \\ 0 & \text{otherwise} \end{cases} \quad (6)$$

$$X_{i,j,c}^{(BL)} = \begin{cases} X_{i,j-l,c} & i-b < H \wedge j-l > 0 \\ 0 & \text{otherwise} \end{cases} \quad (7)$$

$$X_{i,j,c}^{(BR)} = \begin{cases} X_{i,j,c} & i-b < H \wedge j-r < W \\ 0 & \text{otherwise} \end{cases} \quad (8)$$

Figure 1 shows the convolution of a TL padded  $3 \times 3$  image with a  $2 \times 2$  filter is equivalent to a matrix multiplication between convolution matrix  $\mathbf{M}$  and vectored input  $x$ . We leverage this to find the inverse faster. We discuss this in more detail in the subsequent sections. Also padded input  $X^{(TR)}$ ,  $X^{(BL)}$  and  $X^{(BR)}$  are equivalent to  $X^{(TL)}$  once they are flipped along corresponding dimension(s).

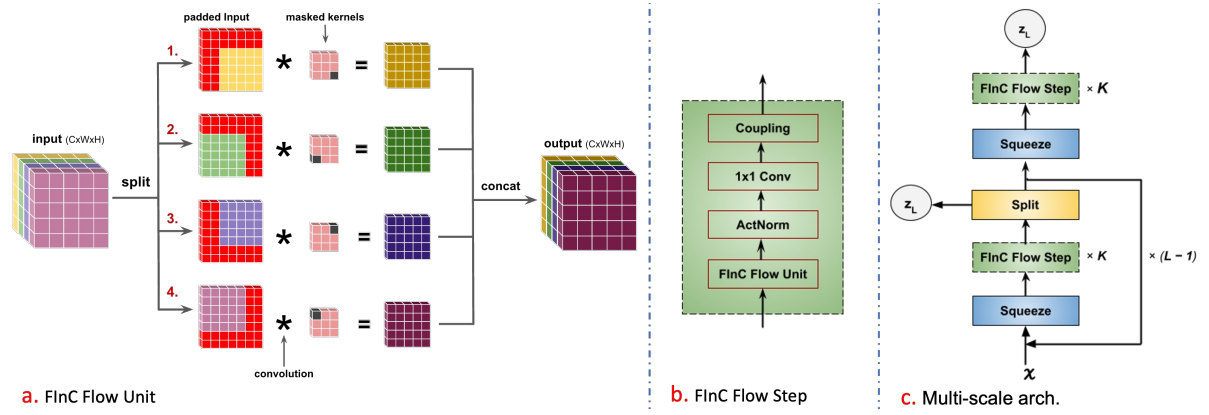


Figure 2: (a) FInC Flow unit: to utilize the independence of convolution on channels the input channels are sliced into four equal parts and then padded (1. top-left, 2. top-right, 3. bottom-right, 4. bottom-left) to keep the input size and output size same. Next, parallelly convoluted each sliced channel with the corresponding masked kernel (masked corner of kernels: 1. bottom-right, 2. bottom-left, 3. top-left, 4. top-right). Finally, concatenate the output from each convolution. (b) We propose a FInC Flow architecture 4.3 where each FInC Flow Step consists of an actnorm step, followed by an invertible  $1 \times 1$  convolution, followed by coupling layer. (c) Flow is combined with a multi-scale architecture 4.4.

Algorithm 1: Fast Parallel Inversion Algorithm of TL padded convolution block(PCB).

```

Input:  $K$ : Kernel of shape  $(C, C, k_H, k_W)$ 
Y: output of the conv of shape  $(C, H, W)$ 
Result:  $X$ : inverse of the conv. with shape  $(C, H, W)$ .
1 Initialization:  $X \leftarrow Y$ ;
2 for  $d \leftarrow 0, H + W - 1$  do
3   for  $c \leftarrow 0, C - 1$  do
4     /* The below lines of code
5     executes parallelly on
6     different threads on GPU
7     for every index  $(c, h, w)$  of
8      $X$  on the  $d$ th diagonal. */
9     for  $k_h \leftarrow 0, k_H - 1$  do
10      for  $k_w \leftarrow 0, k_W - 1$  do
11       for  $k_c \leftarrow 0, C - 1$  do
12        if pixel  $(k_c, h - k_h, w - k_w)$ 
13        not out of bounds then
14          $X[c, h, w] \leftarrow$ 
15          $X[c, h, w] - X[k_c, h -$ 
16          $k_h, w - k_w] * K[c, k_c, k_H - k_h -$ 
17          $1, k_W - k_w - 1];$ 
18        end
19      end
20    end
21  end
22  /* synchronize all threads */
23 end
24 end
    
```

## 4.2 Parallel Inversion Algorithm

We have presented our algorithm in Algorithm 1. The algorithm can be understood using Figure 1.

**Definition 1** (Diagonal Elements). Two pixels  $x_{i,j}$  and  $x_{i',j'}$  are said to be secondary diagonal elements if  $i + i' = j + j'$ . For brevity, we refer to these elements from here on simply as Diagonal Elements.

Theorem 1 proves that every element of on the diagonal can be computed parallelly and Line 2 of the algorithm takes care of that. We initialize  $X$  to  $Y$  in Line 1 and compute  $X$  in Line 8 which is given in Equation 10. It is important that we wait for the threads to synchronize before we move to the next diagonal, as they are needed for computing the elements of the next diagonal. The *not out of bounds* in Line 7 means we are remaining in the  $k \times k$  convolution window and also we are not including pixel  $(i, j)$  while computing  $x_{i,j}$  as given in Equation 10

**Theorem 1.** *The inverse of the pixels on the diagonals of a TL padded convolution can be computed independently and parallelly.*

*Proof.* The  $(i, j)^{th}$  pixel value of the output  $Y$  with shape  $H \times W$  can be calculated as

$$y_{i,j} = (\mathbf{M}_{iW+j,:})^T \cdot x$$

which means  $y_{i,j}$  is the dot product of  $\mathbf{M}_{iW+j,:}$ : i.e., the corresponding row of matrix  $\mathbf{M}$  and the vectored input  $x$ . Because it is a TL padded convolution,  $y_{i,j}$  depends only on the values of  $k \times k$  window of  $x_{\leq i, \leq j}$  pixels where  $x_{\leq i, \leq j}$  are the pixels that are on the top and left side of the pixel  $x_{i,j}$  including  $x_{i,j}$ . Because

all the diagonal values are  $w_{k,k}$ , we have,

$$y_{i,j} = w_{k,k}x_{i,j} + f(x_{<i,<j})$$

$$x_{i,j} = \frac{y_{i,j} - f(x_{<i,<j})}{w_{k,k}}$$

where  $x_{<i,<j}$  are the pixels which are strictly top and left side of  $(i, j)$ . Following the masking pattern of CInC Flow, we have  $w_{k,k} = 1$  and  $f$  is a linear function which is given by weighted sum of the given pixels weighed by the filter values. So,

$$x_{i,j} = y_{i,j} - f(x_{<i,<j}) \quad (9)$$

$$x_{i,j} = y_{i,j} - \sum_{p=0}^k \sum_{q=0}^k x_{i-p,j-q} K_{p,q} \text{ where } p = q \neq 0 \quad (10)$$

Let two pixels  $x_{i,j}$  and  $x_{i',j'}$  be on the same diagonal. This also means that only one of the following settings is true a)  $i < i'$  and  $j > j'$  or b)  $i > i'$  or  $j < j'$ . Either way, we can conclude that computation of  $x_{i,j}$  is not dependent on  $x_{i',j'}$  and vice versa following the result in Equation 9. Hence they can be computed independently. Once  $x_{i,j}$  is computed, following the Equation 9 and the above result, we can compute  $x_{i+1,j}$  and  $x_{i,j+1}$ . Since, the sets of pixels  $x_{<i+1,<j}$  and  $x_{<i,<j+1}$  both include the elements of  $x_{<i,j}$  and also  $x_{i,j}$ , we can write

$$x_{i+1,j} = y_{i+1,j} - f(x_{<i+1,<j})$$

$$= y_{i+1,j} - \alpha x_{i,j} - f_1(x_{<i,<j}) \quad (11)$$

$$x_{i,j+1} = y_{i,j+1} - f(x_{<i,<j+1})$$

$$= y_{i,j+1} - \beta x_{i,j} - f_2(x_{<i,<j}) \quad (12)$$

where  $\alpha$  and  $\beta$  are kernel weights.

From Equations 11 and 12, we can conclude that  $x_{i+1,j}$  and  $x_{i,j+1}$  which are on the same diagonal can be calculated parallelly in a single step.  $\square$

**Theorem 2.** *Algorithm 1 uses only  $(H + W - 1)k^2$  sequential operations.*

*Proof.* We have proved in Theorem 1 that the inverse pixels on a single diagonal can be computed parallelly in one iteration of Algorithm 1. Since there are  $H + W - 1$  number of diagonals in a matrix and there are at maximum  $k^2$  entries in a row of the convolutional matrix, the number of sequential operations needed will be  $(H + W - 1)k^2$ .  $\square$

Thus the running time of our algorithm is  $O(nk^2)$  where  $n = H = W$

### 4.3 FInC Flow Unit

Figure 2a visualizes our  $k \times k$  convolution block. We call this block as FInC Flow *Unit*. We use all the 4 padding techniques mentioned before to different channels of the image. For this purpose, we split the input into four equal parts along the channel axis. We do *TL* padding to the first part, *TR* to the second part, *BL* to the third part and *BR* to the fourth part. Then we use a masked filter on each of these parts to perform the convolution operation parallelly. We call each of this padded image along with its corresponding kernel as Padded Convolution Block (PCB).

### 4.4 Architecture

Figure 2c shows the complete architecture of our model. Our model architecture resembles the architecture of Glow. The multi-scale architecture involves a block of a Squeeze layer, FInC Flow *Step* repeated  $K$  number of times and a Split layer. The whole block is repeated  $L - 1$  number of times. A Squeeze layer follows this and finally FInC Flow *Step* repeated  $K$  times. At the end of each split layer, half of the channels are 'split' (taken away) and modeled as Gaussian distribution samples. These splitted half channels are *latent vectors*. The same is done for the output channels. These are denoted as  $z_L$  in Figure 2(c). Each *FInC Flow Step* consists of a *FInC Flow Unit*, an *Actnorm Layer*, a  $1 \times 1$  Convolutional Layer, followed by a coupling layer.

**Actnorm Layer:** Acts as an activation normalization layer similar to that of a batch normalization layer. Introduced in Glow, this layer performs the affine transformation using scale and bias parameters per channel.

**$1 \times 1$  Convolutional Layer:** This layer introduced in Glow does a  $1 \times 1$  convolution for a given input. Its log determinant and inverse are very easy to compute. It also improves the effectiveness of coupling layers.

**Coupling Layer:** RealNVP introduced a layer in which the input is split into two half. The first half remains unchanged, and the second half is transformed and parameterized by the first half. The output is concatenation of first half and the affine transformation, by functions parameterized by the first, of second half. The inverse and log determinant of coupling layer are computed in a straightforward manner. Coupling layer consists of  $3 \times 3$  convolution followed by a  $1 \times 1$  and a modified  $3 \times 3$  convolution used in Emerging.

**Squeeze:** This layer takes features from spatial to channel dimension (Behrmann et al., 2019), i.e., it reduces the feature dimension by total four, two across

Table 2: Comparison of the bits per dimension (BPD), forward pass time (FT) and sampling time (ST) on standard benchmark datasets of various  $k \times k$  convolution based Normalizing Flow models. FT and ST are presented in seconds.

Model	MNIST			CIFAR-10			Imagenet-32x32			Imagenet-64x64		
	BPD	FT	ST	BPD	FT	ST	BPD	FT	ST	BPD	FT	ST
Emerging	–	0.16	0.62	3.34	0.49	17.19	4.09	0.73	25.79	3.81	1.71	137.04
MaCow	–	–	–	3.16	1.49	3.23	–	–	–	3.69	2.91	8.05
CInC Flow	–	–	–	3.35	0.42	7.91	4.03	0.62	11.97	3.85	1.57	55.71
MintNet	0.98	0.16	17.29	3.32	2.09	230.17	4.06	2.08	230.44	–	–	–
FInC Flow (our)	1.05	0.14	0.09	3.39	0.37	0.41	4.13	0.48	0.52	3.88	1.43	2.11

the height dimension and two across the width dimension resulting in increases the channel dimension by four. As used by (Dinh et al., 2017), we use squeeze layer to reshape the feature maps to have smaller resolution but more channels.

**Split:** Input is split into two halves across the channel dimension. We retain the first half, and a function parameterized by first half transform the second half. The transformed second half is modeled as Gaussian samples, are the *latent vectors*. We do not use the checkerboard pattern used in RealNVP (Dinh et al., 2017) and many others to keep the architecture simple.

## 5 RESULTS

**Bits Per Dimension (BPD):** BPD is closely related to NLLLoss given in equation 2. BPD of  $H \times W \times C$  image is given by

$$\text{bpd} = \frac{\text{NLLLoss} \times \log_2 e}{HWC} \quad (13)$$

Table 2 shows the BPD comparative results of various models with our model. We present the results of MaCow-var which uses Variational Dequantization which was introduced in Flow++ (Ho et al., 2019). BPDs recorded are the reported numbers from the respective model papers.

**Sampling Time:** Table 2 shows the comparative results of our model with other models. For MaCow, we use the official code released by the authors. We use the code for Emerging, which was implemented in PyTorch by the authors of SNF. We have implemented CInC Flow in PyTorch and used it to generate results. The FTs and STs are recorded by averaging ten runs on untrained models (including our model).

In Figure 3, we plot the relationship between the input image size and inverse sampling time. As the input image size increase, our *Parallel Inversion Algorithm* improve by utilizing the independence in the convolution matrix  $M$ . If we input a single image

(batch size = 1), our model performs similarly to the CInC Flow and Emerging. MaCow is far slower because it does the masking of four kernels to maintain the receptive field. To do one convolution, it needs four convolutions to complete one standard convolution, making it slower. Emerging requires two consecutive autoregressive convolutions to have the same receptive field as standard convolution and solver compared to FInC Flow. For batch size = 4 and larger, FInC Flow beats the Emerging, MaCow, and CInC Flow by a big difference (see Figure 3) while maintaining the same receptive field.

### Scaling Sampling Time with Spatial Dimensions:

Table 3 shows the comparison among the invertible convolution-based models. To keep it fair, we restrict the total parameters across all the models to be close to 5 M. We note down the average sampling time (ST) to generate 100 images over ten runs while doubling the size of the sampled image from  $16 \times 16$  all the way to  $128 \times 128$  and also doubling our batch size from 1 all the way to 128. Our model outperforms all the other models in most, if not all, the settings. All the models were untrained and run on a single NVIDIA GTX 1080Ti GPU.

**Image Reconstruction and Generation:** In Figure 4, we present the effectiveness of the FInC Flow model in the reconstruction (sampling) of the images. First, we feed the input image to forward flow and get the *latent vector* ( $z_L$ ). To reconstruct the images from the *latent vector* ( $z_L$ ), give the  $z$  as input to the inverse flow. Figure 4 present the reconstructed face images for the CelebA dataset after training our model for 100 epochs. The model takes a random sample from the Gaussian distribution for the *latent vector* to generate sample images. This *latent vector* is used to generate images by going backward in the flow model. In Figure 5, we present generated sample by our model on the MNIST, CIFAR-10, and ImageNet-64x64 dataset.

Table 3: CIFAR-10: comparison of learnable parameters and the sampling time. FInC Flow has less number of learnable parameters with the same receptive field and fast layers (all the times are averaged over ten loops for  $n = 100$  sample images in seconds). ST = Sample time, FT = Forward Time. MaCow-FG is the fine-grained MaCow model and MaCow-org stands for MaCow model utilizes the original multi-scale architecture which is the same as Glow. MaCow and our method is closely similar in term of the convolutional design. So, here we show that our proposed method do fast sampling while maintaining the faster forward time.

Models	Setting (K and L)	Learnable params (M = million)	FT(n=100)	ST(n=100)
MaCow-FG	[4, [12, 12], [12, 12], 12]	37.19M	0.88	2.64
MaCow-org	[4, [12, 12], [12, 12], 12], [4, 4]	38.4M	1.48	3.23
FInC Flow (our)	[28, 28, 28]	39.46M	<b>0.37</b>	<b>0.41</b>

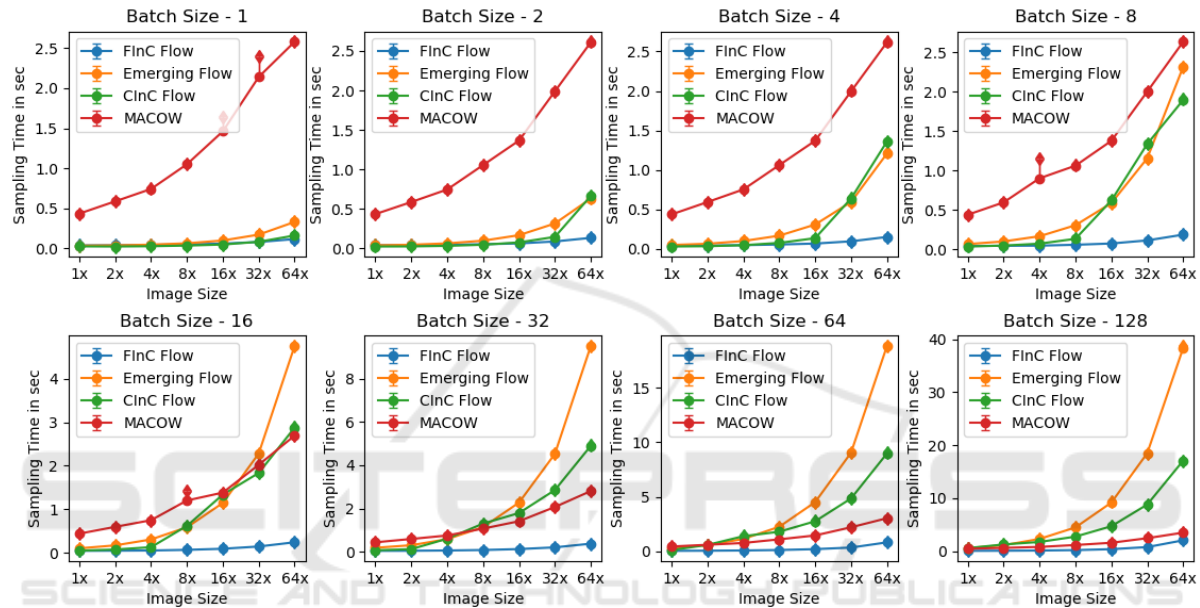


Figure 3: Sampling Times for four models - our, Emerging, CInC Flow, MaCow. Each plot gives the 95% Confidence Interval (CI) time of the ten runs to sample 100 images. X-axis represents the sizes of the image sampled starting from  $16 \times 16 \times 2$  ( $H \times W \times C$ ) all the way to  $128 \times 128 \times 2$ .



Figure 4: Comparison of (a) original and (b) reconstructed image samples for the  $64 \times 64$  CelebA dataset after FInC Flow model for 100 epochs. From the images, we can conclude our model reconstruct original image.



Figure 5: Uncurated generated samples images from our flow model.

## 6 CONCLUSION

With a parallel inversion approach, we present a  $k \times k$  invertible convolution for Normalizing flow models. We utilize it to develop a model with highly efficient sampling pass, normalizing flow architecture. We implement our parallel algorithm on GPU and presented benchmarking results, which show a significant enhancement in forward and sampling speeds when compared to alternative methods for  $k \times k$  invertible convolution.

## REFERENCES

- Behrmann, J., Grathwohl, W., Chen, R. T., Duvenaud, D., and Jacobsen, J.-H. (2019). Invertible residual networks. In *International Conference on Machine Learning*, pages 573–582. PMLR.
- Brock, A., Donahue, J., and Simonyan, K. (2019). Large scale GAN training for high fidelity natural image synthesis. In *International Conference on Learning Representations*.
- Deng, L. (2012). The mnist database of handwritten digit images for machine learning research. *IEEE Signal Processing Magazine*, 29(6):141–142.
- Dinh, L., Krueger, D., and Bengio, Y. (2014). Nice: Non-linear independent components estimation. *arXiv preprint arXiv:1410.8516*.
- Dinh, L., Sohl-Dickstein, J., and Bengio, S. (2017). Density estimation using real nvp. In *International Conference on Learned Representations*.
- Goodfellow, I., Pouget-Abadie, J., Mirza, M., Xu, B., Warde-Farley, D., Ozair, S., Courville, A., and Bengio, Y. (2014a). Generative adversarial nets. In Ghahramani, Z., Welling, M., Cortes, C., Lawrence, N., and Weinberger, K., editors, *Advances in Neural Information Processing Systems*, volume 27. Curran Associates, Inc.
- Goodfellow, I., Pouget-Abadie, J., Mirza, M., Xu, B., Warde-Farley, D., Ozair, S., Courville, A., and Bengio, Y. (2014b). Generative adversarial nets. *Advances in neural information processing systems*, 27.
- Hazami, L., Mama, R., and Thurairatnam, R. (2022). Efficient-ldvae: Less is more. *arXiv preprint arXiv:2203.13751*.
- Ho, J., Chen, X., Srinivas, A., Duan, Y., and Abbeel, P. (2019). Flow++: Improving flow-based generative models with variational dequantization and architecture design. In *International Conference on Machine Learning*, pages 2722–2730. PMLR.
- Ho, J., Jain, A., and Abbeel, P. (2020). Denoising diffusion probabilistic models. *Advances in Neural Information Processing Systems*, 33:6840–6851.
- Hoogeboom, E., Van Den Berg, R., and Welling, M. (2019). Emerging convolutions for generative normalizing flows. In *International Conference on Machine Learning*, pages 2771–2780. PMLR.
- Keller, T. A., Peters, J. W., Jaini, P., Hoogeboom, E., Forré, P., and Welling, M. (2021). Self normalizing flows. In *International Conference on Machine Learning*, pages 5378–5387. PMLR.
- Kingma, D. P. and Ba, J. (2015). Adam: A method for stochastic optimization. In Bengio, Y. and LeCun, Y., editors, *3rd International Conference on Learning Representations, ICLR 2015, San Diego, CA, USA, May 7-9, 2015, Conference Track Proceedings*.
- Kingma, D. P. and Dhariwal, P. (2018). Glow: Generative flow with invertible 1x1 convolutions. *Advances in neural information processing systems*, 31.
- Kingma, D. P. and Welling, M. (2013). Auto-encoding variational bayes. *arXiv preprint arXiv:1312.6114*.
- Kingma, D. P., Welling, M., et al. (2019). An introduction to variational autoencoders. *Foundations and Trends® in Machine Learning*, 12(4):307–392.
- Kobyzev, I., Prince, S. J., and Brubaker, M. A. (2020). Normalizing flows: An introduction and review of current methods. *IEEE transactions on pattern analysis and machine intelligence*, 43(11):3964–3979.
- Krizhevsky, A. (2009). Learning multiple layers of features from tiny images.
- Liu, Z., Luo, P., Wang, X., and Tang, X. (2015). Deep learning face attributes in the wild. In *Proceedings of the IEEE international conference on computer vision*, pages 3730–3738.
- Lu, Y. and Huang, B. (2020). Woodbury transformations for deep generative flows. *Advances in Neural Information Processing Systems*, 33:5801–5811.
- Ma, X., Kong, X., Zhang, S., and Hovy, E. (2019). Macow: Masked convolutional generative flow. *Advances in Neural Information Processing Systems*, 32.
- Meng, C., Zhou, L., Choi, K., Dao, T., and Ermon, S. (2022). Butterflyflow: Building invertible layers with butterfly matrices. In *International Conference on Machine Learning*, pages 15360–15375. PMLR.
- Nagar, S., Dufraisse, M., and Varma, G. (2021). CInc flow: Characterizable invertible 3x3 convolution. In *The 4th Workshop on Tractable Probabilistic Modeling*.
- Nash, C., Ganin, Y., Eslami, S. A., and Battaglia, P. (2020). Polygen: An autoregressive generative model of 3d meshes. In *International conference on machine learning*, pages 7220–7229. PMLR.
- Oord, A. v. d., Dieleman, S., Zen, H., Simonyan, K., Vinyals, O., Graves, A., Kalchbrenner, N., Senior, A., and Kavukcuoglu, K. (2016). Wavenet: A

- generative model for raw audio. *arXiv preprint arXiv:1609.03499*.
- Rezende, D. and Mohamed, S. (2015). Variational inference with normalizing flows. In *International conference on machine learning*, pages 1530–1538. PMLR.
- Russakovsky, O., Deng, J., Su, H., Krause, J., Satheesh, S., Ma, S., Huang, Z., Karpathy, A., Khosla, A., Bernstein, M., et al. (2015). Imagenet large scale visual recognition challenge. *International journal of computer vision*, 115(3):211–252.
- Song, Y., Durkan, C., Murray, I., and Ermon, S. (2021a). Maximum likelihood training of score-based diffusion models. *Advances in Neural Information Processing Systems*, 34:1415–1428.
- Song, Y. and Ermon, S. (2019). Generative modeling by estimating gradients of the data distribution. *Advances in Neural Information Processing Systems*, 32.
- Song, Y., Meng, C., and Ermon, S. (2019). Mintnet: Building invertible neural networks with masked convolutions. *Advances in Neural Information Processing Systems*, 32.
- Song, Y., Sohl-Dickstein, J., Kingma, D. P., Kumar, A., Ermon, S., and Poole, B. (2021b). Score-based generative modeling through stochastic differential equations. In *International Conference on Learning Representations*.
- Zhang, D., Malkin, N., Liu, Z., Volokhova, A., Courville, A., and Bengio, Y. (2022). Generative flow networks for discrete probabilistic modeling. In Chaudhuri, K., Jegelka, S., Song, L., Szepesvari, C., Niu, G., and Sabato, S., editors, *Proceedings of the 39th International Conference on Machine Learning*, volume 162 of *Proceedings of Machine Learning Research*, pages 26412–26428. PMLR.

## ADDITIONAL DETAILS

Code to our implementation is available here: <https://github.com/aditya-v-kallappa/FInCFlow>

**Datasets.** We train our model on standard benchmark datasets MNIST (Deng, 2012), CIFAR-10 (Krizhevsky, 2009), and ImageNet (Russakovsky et al., 2015) sampled down to  $32 \times 32$  and  $64 \times 64$ . We also train our model on CelebA (Liu et al., 2015) sampled down to  $64 \times 64$ . Figure 4a present the CelebA- $64 \times 64$  reconstructed samples and Figure 5b for the CIFAR-10 and ImageNet- $64 \times 64$  generated samples.

**Hyperparameters.** To train our model, we use Adam optimizer (Kingma and Ba, 2015) with learning rate of 0.001 with an exponential decay of 0.99997 per epoch. For training on Imagenet, we also make sure that the gradients stay between  $-1$  and  $+1$  by clipping them.

**Masking** To make sure the masked values in the Padded Conv Blocks, we ensure they are not affected by back propagation. To achieve this, we reset the gradients of the masked values to zero after every training iteration.

**Cuda Code Details.** To run CUDA code, we use PyTorch-LTS 1.8.2 and cudatoolkit 10.2. While we can implement Algorithm 2 to find inverse of each padded block individually, we can take advantage of the fact that all 4 Padded Conv Blocks are equivalent after proper flipping of padded inputs and kernels. This is done by using Algorithm 2 on GPU.

First we split  $Y$  into 4 parts across channel dimension following the architecture shown in 2. This is given in Line 1. Then we flip  $Y$  and kernels to match TL-padding which is given in Line 2. Then we concatenate them to get the final  $Y$  and  $K$  respectively which are given in Lines 3 and 4. Then we apply Algorithm 2 to find the inverse. We do the reverse process of the above to get the correct  $X$ . The steps are given in Lines 5, 6, 7, 8.

We fix the number of threads of each grid of the GPU to be 1024, the number of  $grids_x$  to be the batch size and  $grids_y$  to be 4 which is the number of Padded Conv Blocks in a single FInC Flow Unit. This ensures that not only GPU inverts the whole FInC Flow Unit at once but also on a batch of images.

---

Algorithm 2: Fast Parallel Inversion Algorithm for FInC Flow Unit.

---

**Input:**  $K_1, K_2, K_3, K_4$  - Convolution Kernels of different PCB,  $Y$  - Output of the FInC Flow Unit

**Result:**  $X$  - Input to the FInC Flow Unit / Inverse of the FInC Flow Unit

1.  $Y_1, Y_2, Y_3, Y_4 \leftarrow split(Y)$
  2. Flip  $Y_2, Y_3, Y_4, K_2, K_3, K_4$  (inplace) appropriately to match TL padding
  3.  $X \leftarrow concat(Y_1, Y_2, Y_3, Y_4)$
  4.  $K \leftarrow concat(K_1, K_2, K_3, K_4)$
  5. Apply Algorithm 1 with input  $K, Y$  to get  $X$
  6.  $X_1, X_2, X_3, X_4 \leftarrow split(X)$
  7. Flip  $X_2, X_3, X_4$  appropriately to get the correct output
  8.  $X \leftarrow concat(X_1, X_2, X_3, X_4)$
- 

**Running MaCow, Emerging, CInC Flow, SNF.** For MaCow and SNF, we use the official code re-

leased by the authors. Emerging was implemented in PyTorch by the authors of SNF. We make use of that. We have implemented CInC Flow on PyTorch to get the results.

#### **Computing Run-time and Confidence Intervals.**

We run the model (both forward and sampling) 11 times and ignore the 1<sup>st</sup> run as it includes the initialization time. We calculate the mean, standard deviation and 95% confidence interval and plot the numbers.

To calculate forward time, we pass 100 images, as for sampling times, we sample 100 images. We present these numbers in Table-3.

For sampling time comparison of different models shown in Figure 3, we set the total number of parameters for all the models to be close to 5M to make it a fair comparison.

**Hardware/Training Time.** Our hardware setup consists of Intel Xeon E5-2640 v4 processor providing 40 cores, 80 GB of DDR4 RAM, 4 Nvidia GeForce GTX 1080 Ti GPUs each with 12 GB of VRAM. We train our model on all GPUs using PyTorch's Data Parallel class. We implement early stopping mechanism for smaller datasets like MNIST, CIFAR-10. For others we train the model for a maximum epochs. To evaluate Forward Time and Sampling Time, we use only one of the GPUs. We evaluate our FInC Flow model on MNIST, CIFAR-10, Imagenet-32x32, and Imagenet-64x64 datasets for three metrics - (a) Loss expressed in Bits per Dimension (BPD), (b) Forward Pass Time (FT): Time taken for 100 images to be passed through the model and (c) Sampling Time(ST): Time taken by the model to generate 100 images. To do this, we train our model with Adam Optimizer with a learning rate ( $lr$ ) of 0.001 and exponentially reduce the  $lr$  by 0.99997 after each epoch. We have used 4 NVIDIA GTX 1080 Ti GPUs to train our model. Evaluation(FT/ST) is done on a single GPU.